

# Surface modified SPIONs-Cr(VI) ions-immobilized organic-inorganic hybrid as a magnetically recyclable nanocatalyst for rapid synthesis of polyhydroquinolines under solvent-free conditions at room temperature

Ali Maleki  | Reivar Hamidi | Saied Maleki | Jamal Rahimi

Catalysts and Organic Synthesis Research Laboratory, Department of Chemistry, Iran University of Science and Technology, Tehran 16846-13114, Iran

## Correspondence

Ali Maleki, Catalysts and Organic Synthesis Research Laboratory, Department of Chemistry, Iran University of Science and Technology, Tehran 16846-13114, Iran.  
Email: maleki@iust.ac.ir

In this work, a magnetic hybrid dichromate nanocomposite with triphenylphosphine surface modified superparamagnetic iron oxide nanoparticles (SPIONs) as a recyclable nanocatalyst was designed, prepared and characterized by Fourier transform infrared spectroscopy (FT-IR) spectra, X-ray diffraction (XRD) pattern analysis, vibrating sample magnetometer (VSM) curves, X-ray fluorescence (XRF) analysis, thermogravimetric analysis (TGA), scanning electron microscopy (SEM) and transmission electron microscopy (TEM) images and dynamic light scattering (DLS) analysis. Then, it was used in a green and efficient procedure for one-pot multicomponent synthesis of polyhydroquinoline derivatives by the condensation of aldehydes, dimedone or 1,3-cyclohexadione, ethyl acetoacetate and ammonium acetate. This protocol includes some new and exceptional advantages such as short reaction times, low catalyst loading, high yields, solvent-free and room temperature conditions, easy separation and reusability of the catalyst.

## KEYWORDS

Fe<sub>3</sub>O<sub>4</sub> nanocomposite, green conditions, heterogeneous nanocatalyst, multicomponent reaction, polyhydroquinoline

## 1 | INTRODUCTION

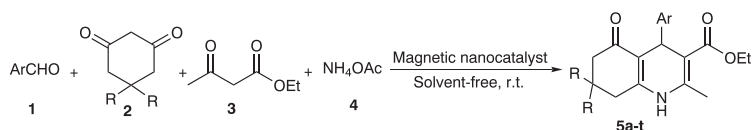
Nowadays, multicomponent reaction is not an unfamiliar topic to the chemists and pharmacists. From the beginning of its introduction to the scientific world, it has drawn enormous attention to itself due to its exceptional advantages in comparison to conventional procedures, the advantages that tempts every scientist in chemistry and pharmacy to use it in the various compounds synthesis. Chemists and pharmacists implement multicomponent reactions method significantly because in this way they are able to achieve their targets in brief time and also they could save material, energy and money.<sup>[1]</sup>

Polyhydroquinoline and 1,4-dihydropyridine derivatives include a broad spectrum of pharmacologically active compounds that, in recent years, have drawn much attention to themselves because of their diverse pharmacological and therapeutic properties such as vasodilator, hepatoprotective, antiatherosclerotic, bronchodilator, antitumor, geroprotective and antidiabetic activities.<sup>[2-8]</sup> Therefore, various methods have been reported for their synthesis because of their biological, industrial and synthetic importance. However, most of these methods have significant disadvantages, the use of high temperatures, expensive metal precursors, environmentally harmful catalysts, harsh reaction conditions, long reaction times

and large quantity of volatile organic solvents limit the implementation of these techniques. In addition, in most of the reported methods, catalysts are damaged in the work-up process and cannot be recovered and reused. Consequently, the design of efficient and recoverable catalysts for the synthesis of and polyhydroquinolines seems to be essential. One method that is considered an environmentally benign process is the designing of the heterogeneous catalysts because these systems are easy to handle, recover and are green processes.<sup>[9]</sup>

Nanoparticles are much more reactive than the particulate metal counterpart because catalysis happens on metal surface. Therefore, due to small sizes and large surface areas of nanoparticles, heterogeneous catalysts are often used in the form of nanoparticles. In recent decade, SPIONs, as a main group of separation materials, has drawn significant attention to itself in chemistry and material science, due to its crucial applications in manufacturing catalysts for the synthesis of various biological active compounds. In addition, SPIONs has excellent properties such as magnetism and insolubility that enable the catalyst to be easily separated with an external magnetic field and reused frequently without considerable loss of catalytic activity.<sup>[10–19]</sup>

In continuation of our recent works in order to applying heterogeneous nanocatalysts in organic synthesis,<sup>[20,21]</sup> herein, a magnetic dichromate hybrid with triphenylphosphine surface modified SPIONs,  $\text{Fe}_3\text{O}_4@\text{SiO}_2@\text{PPh}_3@\text{Cr}_2\text{O}_7^{2-}$  as a recoverable and efficient composite nanocatalyst is prepared and used for the synthesis of polyhydroquinolines **5a-t** via a multicomponent reaction of various aldehydes **1**, dimedone or 1,3-cyclohexadione **2**, ethyl acetoacetate **3** and ammonium acetate **4** under solvent-free conditions at room temperature (Scheme 1). Although some recent works dealing with the catalytic synthesis of polyhydroquinoline and dihydropyridine derivatives using magnetic nanoparticles,<sup>[22–26]</sup> but, this method can be considered as a greener approach for the efficient and rapid synthesis of biologically active substituted polyhydroquinolines by using a recyclable nanocatalyst under mild reaction conditions. To the best of our knowledge, the present report can be regarded as a new and first solvent-free and room temperature protocol for the synthesis of polyhydroquinolines catalyzed by a hybrid nanocomposite.



**SCHEME 1** Synthesis of polyhydroquinolines **5a-t**

## 2 | RESULTS AND DISCUSSION

### 2.1 | Characterization of the magnetite nanocatalyst

#### 2.1.1 | FT-IR spectrum of the prepared nanocatalyst

To confirm the preparation of magnetite-dichromate nanomaterials, the FT-IR spectrum of the prepared nanocatalyst was obtained. As shown in Figure 1, bands centered at 584, 635, 797, 1097, 810, 2930, 2984, 770, 805, 895, 915 ( $\nu_{\text{asymmetric Cr=O}} (A_1)$ ),  $954 \text{ cm}^{-1}$  ( $\nu_{\text{symmetric Cr=O}} (E)$ ) approved the preparation of the magnetite nanocatalyst.

#### 2.1.2 | XRD pattern analysis of the magnetite nanocatalyst

To study the structure and phase purity of the magnetite nanocatalyst X-ray diffraction patterns (XRD) were used. The sharp peaks in the XRD patterns verified good crystallinity of the prepared samples (Figure 2). The results are in agreement with standard patterns of inverse cubic spinel magnetite ( $\text{Fe}_3\text{O}_4$ ) crystal structure (JCPDS No. 19-0629) showing eight diffraction peaks at  $2\theta$  about  $18.17^\circ$ ,  $30.24^\circ$ ,  $35.64^\circ$ ,  $43.39^\circ$ ,  $53.69^\circ$ ,  $57.20^\circ$ ,  $62.95^\circ$  and  $74.25^\circ$  corresponding to (1 1 1), (2 2 0), (3 1 1), (4 0 0), (4 2 2), (5 1 1), (4 4 0) and (5 3 3). The crystallite sizes were calculated using Scherrer's formula. The crystallite size of the magnetite nanocatalyst was about 19.3 nm according to the XRD peak at  $35.64^\circ$ .

#### 2.1.3 | SEM image of the magnetite nanocatalyst

Scanning electron microscopy (SEM) image was used to study the morphology and particle size distribution in the surface of the nanostructured nanocatalyst (Figure 3). The SEM image illustrated that the magnetite nanocatalyst particles are spherical with a mean diameter of 25 nm with uniform size and good dispersity.

#### 2.1.4 | Thermal stability properties of the nanocatalyst

The thermal stability and composition ratio in the obtained nanocomposite was measured through the TGA under air

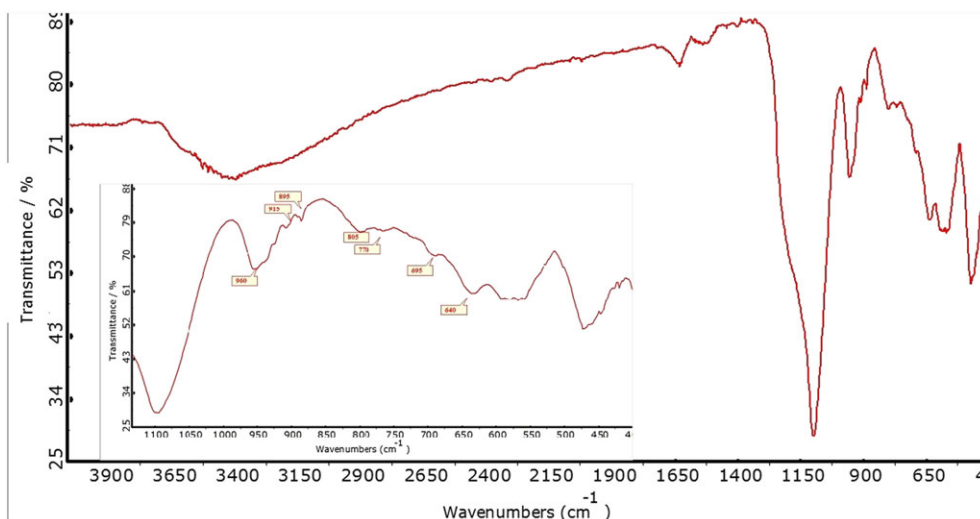


**FIGURE 1** FT-IR spectrum of the magnetite nanocatalyst

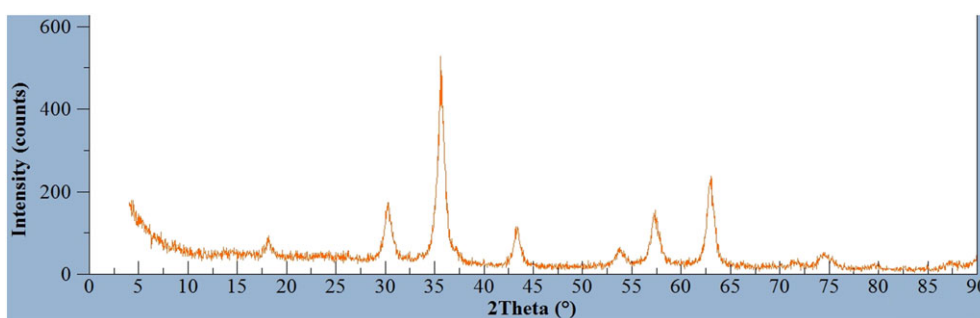


**FIGURE 2** XRD pattern of the magnetite nanocatalyst

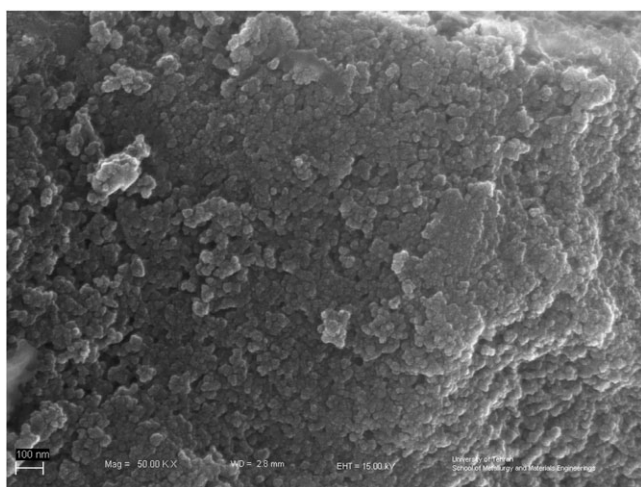


**FIGURE 3** SEM image of the magnetite nanocatalyst

atmosphere with heating rate of  $10^{\circ}\text{C min}^{-1}$  within temperature range of  $0\text{--}800^{\circ}\text{C}$ . As illustrated in Figure 4, the TGA-DTA and mass loss curves depicting the variations of the residual masses of the samples with temperature. The organic material and magnetite of the sample were completely burned to generate gas products and converted

into iron oxides at the elevated temperature, respectively. The composition ratio of the nanocomposite can be estimated from the residual mass percentage. The magnetic content was about 20%. The first weight loss stage (below  $100^{\circ}\text{C}$ ) can be ascribed to the evaporation of water molecules in the composition. The next weight loss stage was started from about  $400$  to complete at  $700^{\circ}\text{C}$  that was because of the decomposition of the core/shell. No further obvious decomposition exhibits a high thermal stability in comparison with similar structures.

### 2.1.5 | Magnetic properties of the magnetite nanocatalyst

The magnetic property of the nanocomposite was characterized using a vibrating sample magnetometer (VSM) at room temperature. The magnetization curves for SPIONs,  $\text{Fe}_3\text{O}_4@\text{SiO}_2$  and  $\text{Fe}_3\text{O}_4@\text{SiO}_2@\text{PPh}_3@\text{Cr}_2\text{O}_7$  nanoparticles did not show hysteresis in the magnetization for the three types of nanoparticles. In addition, neither coercivity nor remanence was observed which suggested that the three nanoparticles were

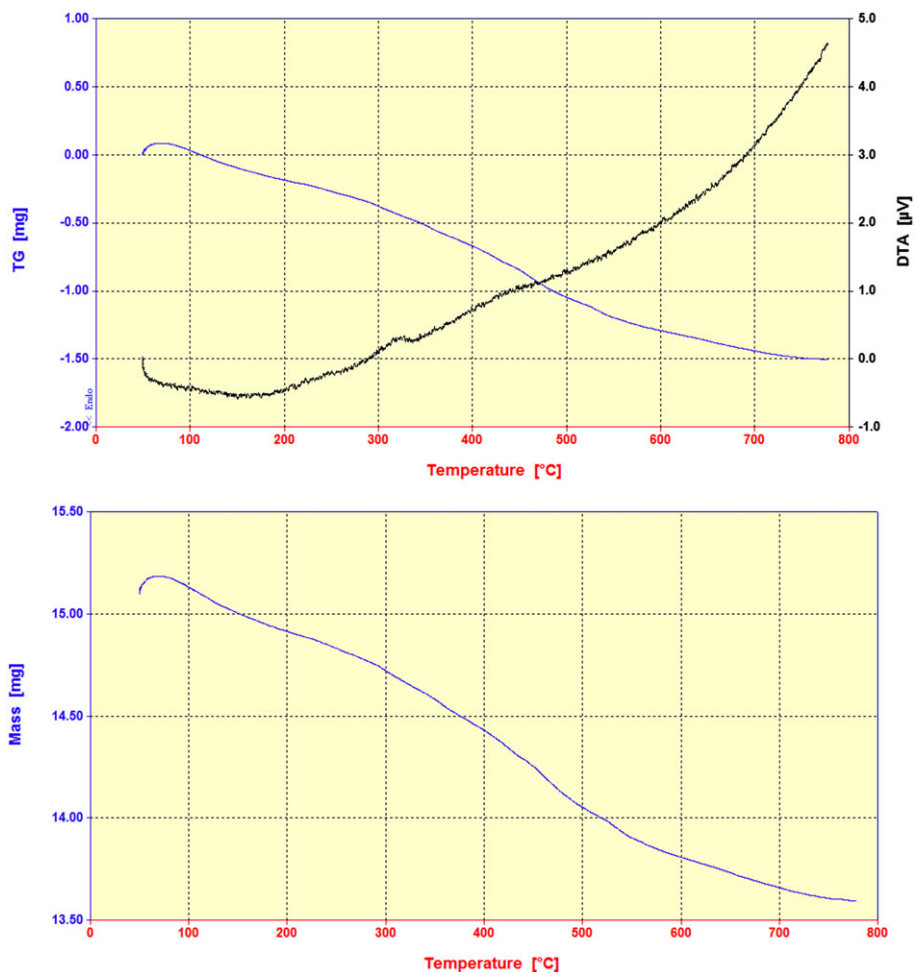


**FIGURE 4** TGA-DTA of the nanocomposite

superparamagnetic. The measured saturation magnetizations were about  $54 \text{ emu g}^{-1}$  for SPIONs, about  $40 \text{ emu g}^{-1}$  for  $\text{Fe}_3\text{O}_4/\text{SiO}_2$  and about  $29 \text{ emu g}^{-1}$  for the magnetite nanocatalyst. The saturation magnetization significantly decreased after preparation of core-shell

$\text{Fe}_3\text{O}_4/\text{SiO}_2$  and nanocatalyst. However, the prepared the magnetite nanocatalyst still maintained good magnetic properties and could be completely and quickly separated from the reaction medium easily by a magnet.

Furthermore, for the measurement of the quantity of chromium XRF analysis was used. According to the results, the quantity of chromium was approximately 2.5%. Therefore, the immobilization of  $\text{Cr}_2\text{O}_7^{2-}$  was equal with  $0.03 \text{ mol}/100 \text{ g}$ .

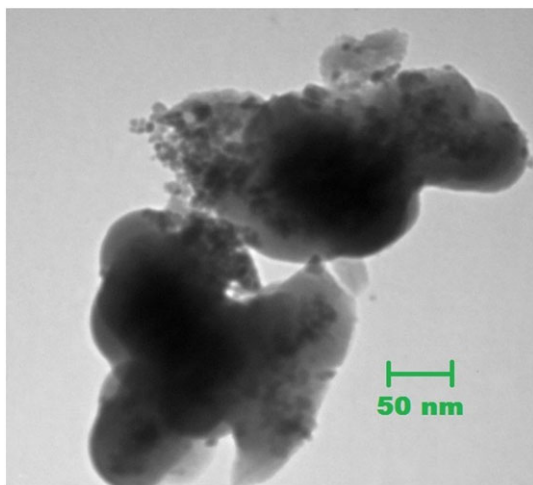


**FIGURE 5** TEM image of the  $\text{Fe}_3\text{O}_4/\text{SiO}_2$  core/shell

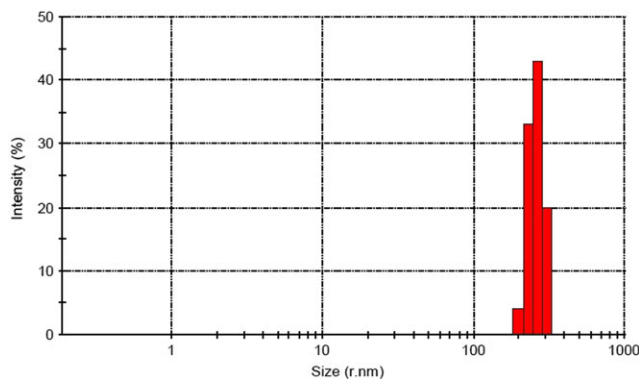


**FIGURE 6** DLS analysis of the nanocomposite

Transmission electron microscopy (TEM) image was used to confirm the core/shell morphology in the nanostructure including Fe<sub>3</sub>O<sub>4</sub> as dark core and SiO<sub>2</sub> light shell (Figure 5).

To study the particle size distribution vs intensity, dynamic light scattering (DLS) analysis was provided. As can be seen in Figure 6, after immobilization of the next two shells on the Fe<sub>3</sub>O<sub>4</sub>@SiO<sub>2</sub> core/shell, the particles' diameter has been increased to higher than 100 nm.

**TABLE 1** Optimization of the reaction conditions in the synthesis of **5d** at room temperature

Entry	Solvent	Catalyst (g)	Time (min)	Yield <sup>a</sup> (%)
1	-	-	240	<40
2	-	0.02	20	80
3	-	0.003	20	95
4	-	0.004	20	95
5	-	0.008	20	91
6	C <sub>2</sub> H <sub>5</sub> OH	0.003	45	89
7	H <sub>2</sub> O	0.003	70	55
8	CH <sub>3</sub> CN	0.003	90	60
9	CH <sub>2</sub> Cl <sub>2</sub>	0.003	80	65

<sup>a</sup>Isolated yields.

Therefore, this DLS can be another evidence for the claim of multilayer nanostructure formation.

## 2.2 | Catalytic performance of the magnetite nanocatalyst

To investigate the effect of solvent, the condensation reaction of an equimolar amount of 4-chlorobenzaldehyde, dimedone, ethyl acetoacetate, and ammonium acetate in H<sub>2</sub>O, CH<sub>3</sub>CN, CH<sub>2</sub>Cl<sub>2</sub>, C<sub>2</sub>H<sub>5</sub>OH and under solvent-free conditions at room temperature using 0.003 g of the magnetite nanocatalyst was carried out to produce the specified product **5d** (Table 1). The optimized condition was the solvent-free condition; because, it was performed in short reaction time and in excellent yield. To the best of our knowledge, the resulted yield and time for this reaction could not be obtained under similar reaction conditions, neither in the absence of any catalyst nor other catalysts which have been used yet. Therefore, it can be said that the prepared catalyst plays an important role in the reaction which lead to the synthesis of polyhydroquinoline derivatives.

To investigate the catalytic performance of the magnetite nanocatalyst, a pilot experiment was implemented. This experiment was done by the reaction of an

**TABLE 2** Synthesis of polyhydroquinolines **5a-t** in the presence of the nanocatalyst under solvent-free conditions at room temperature

Entry	Ar	R <sup>1</sup>	R <sup>2</sup>	Product	Time (min)	Yield <sup>a</sup> (%)
1	C <sub>6</sub> H <sub>5</sub>	CH <sub>3</sub>	CH <sub>3</sub>	<b>5a</b>	25	90
2	4-MeOC <sub>6</sub> H <sub>4</sub>	CH <sub>3</sub>	CH <sub>3</sub>	<b>5b</b>	10	90
3	4-MeC <sub>6</sub> H <sub>4</sub>	CH <sub>3</sub>	CH <sub>3</sub>	<b>5c</b>	11	91
4	4-ClC <sub>6</sub> H <sub>4</sub>	CH <sub>3</sub>	CH <sub>3</sub>	<b>5d</b>	20	95
5	2-ClC <sub>6</sub> H <sub>4</sub>	CH <sub>3</sub>	CH <sub>3</sub>	<b>5e</b>	20	87
6	4-OHC <sub>6</sub> H <sub>4</sub>	CH <sub>3</sub>	CH <sub>3</sub>	<b>5f</b>	15	82
7	3-OHC <sub>6</sub> H <sub>4</sub>	CH <sub>3</sub>	CH <sub>3</sub>	<b>5g</b>	15	90
8	4-NO <sub>2</sub> C <sub>6</sub> H <sub>4</sub>	CH <sub>3</sub>	CH <sub>3</sub>	<b>5h</b>	25	80
9	2,4-Cl <sub>2</sub> -C <sub>6</sub> H <sub>3</sub>	CH <sub>3</sub>	CH <sub>3</sub>	<b>5i</b>	20	92
10	4-OH-3-MeOC <sub>6</sub> H <sub>4</sub>	CH <sub>3</sub>	CH <sub>3</sub>	<b>5j</b>	25	95
11	2-OH-4,6-MeOC <sub>6</sub> H <sub>2</sub>	CH <sub>3</sub>	CH <sub>3</sub>	<b>5k</b>	20	95
12	4-BrC <sub>6</sub> H <sub>4</sub>	CH <sub>3</sub>	CH <sub>3</sub>	<b>5l</b>	21	95
13	4-CNC <sub>6</sub> H <sub>4</sub>	CH <sub>3</sub>	CH <sub>3</sub>	<b>5m</b>	25	92
14	Thiophen-2-carbaldehyde	CH <sub>3</sub>	CH <sub>3</sub>	<b>5n</b>	15	93
15	Furan-2-carbaldehyde	CH <sub>3</sub>	CH <sub>3</sub>	<b>5o</b>	15	91
16	4-MeOC <sub>6</sub> H <sub>4</sub>	H	H	<b>5p</b>	8	95
17	4-MeC <sub>6</sub> H <sub>4</sub>	H	H	<b>5q</b>	9	95
18	4-ClC <sub>6</sub> H <sub>4</sub>	H	H	<b>5r</b>	15	98
19	4-OHC <sub>6</sub> H <sub>4</sub>	H	H	<b>5s</b>	15	90
20	Thiophen-2-carbaldehyde	H	H	<b>5t</b>	10	95

<sup>a</sup>Isolated yields.

aldehyde, dimedone or 1,3-cyclohexadione, ethyl acetoacetate, and ammonium acetate in the presence of a catalytic amount of the magnetite nanocatalyst under solvent-free conditions at room temperature to afford polyhydroquinolines **5a-t** (yield = 80-95%). As indicated in Table 2, the reaction was carried out successfully with a wide range of aromatic and heteroaromatic aldehydes carrying either electron-donating or electron-withdrawing substituent in the *ortho*, *meta*, and *para* positions.

The main advantage of heterogeneous solid catalysts in organic transformations is their reusability. The present nanocatalyst was readily recovered from the reaction mixture as outlined in the experimental section. The separated catalyst was washed with ethanol, dried and reused in the subsequent reactions at least five times without significant reduction in its activity. For example, the reaction

of 4-chlorobenzaldehyde with dimedone, **3** and **4** in the presence of the magnetite nanocatalyst (0.003 g) gave the product ethyl 2,7,7-trimethyl-4-(4-chlorophenyl)-5-oxo-1,4,5,6,7,8-hexahydroquinoline-3-carboxylate **5d** in 95% yield at room temperature. The results are summarized in Figure 7.

A proposed mechanism for the synthesis of polyhydroquinolines in the presence of the magnetite nanocatalyst is shown in Scheme 2. First, the magnetite nanocatalyst catalyzes the reaction of aldehydes **1** or  $\text{NH}_4\text{OAc}$  **4** with active methylene compounds **2** or **3** to give intermediates **6** and **7** or **8** and **9** via Knoevenagel condensations and imine formations. Then, a Michael-type addition between them and then following by an intramolecular nucleophilic attack of  $\text{NH}_2$  groups of enamine forms to one of the carbonyl sites give the

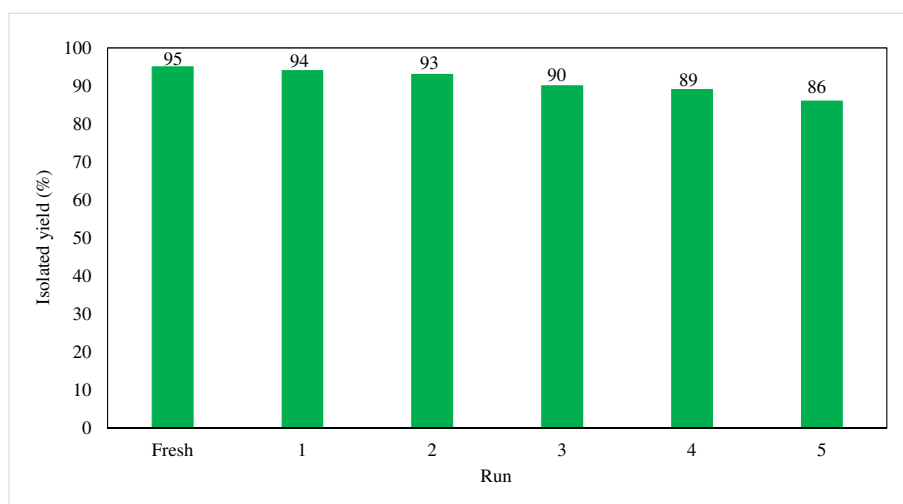
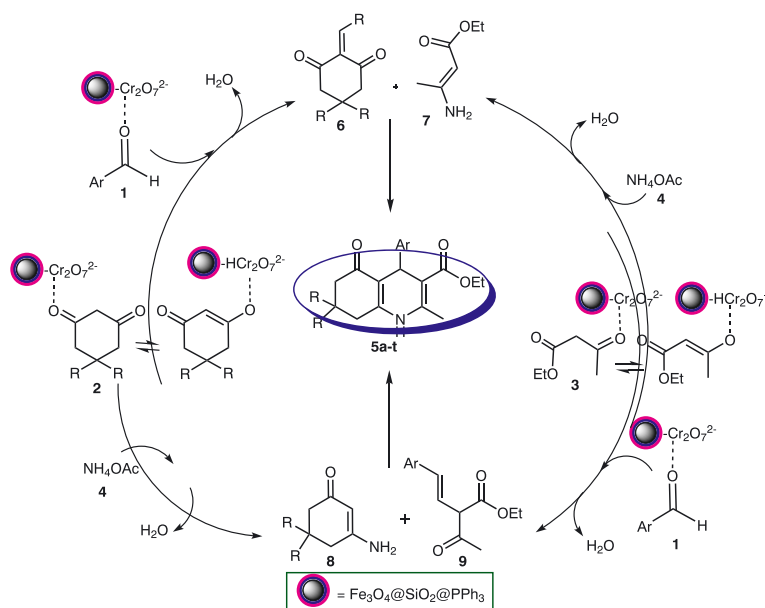


FIGURE 7 Reusability study of the magnetite nanocatalyst in the synthesis of **5d**



SCHEME 2 The proposed mechanism for the synthesis of polyhydroquinolines in the presence of the magnetite nanocatalyst

products **5a-t**. It was suggested that the role of  $\text{Cr}_2\text{O}_7^{2-}$  ions of the nanocatalyst can be regarded as an acid-base reaction between CH-acid of the methylene compounds **2** or **3** and  $\text{Cr}_2\text{O}_7^{2-}$  ions of the nanocatalyst. As can be seen, it was carried out via proton transfer mechanism not an electron transferring path. Because, oxidized aromatic pyridine cores did not form on the obtained products.

### 3 | CONCLUSIONS

In summary, we have introduced an efficient preparation, identification and catalytic performance of magnetic dichromate hybrid nanoparticles with triphenylphosphine surface modified iron oxide in a four-component condensation reaction for the synthesis of polyhydroquinoline derivatives starting from simple and readily available precursors by using under solvent-free conditions at room temperature. A large number of unique properties of this catalyst were also observed including short reaction times, easy workup procedure, significant reusability of the catalyst, high atom economy, excellent yields and environmentally benign reaction conditions.

### 4 | EXPERIMENTAL

#### 4.1 | General

All chemicals were purchased from Merck, Fluka and Sigma-Aldrich, and used without further purification. All reactions and the purity of polyhydroquinolines were monitored by thin-layer chromatography (TLC) using aluminum plates coated with silica gel F254 plates (Merck) using ethyl acetate and *n*-hexane as eluents. The spots were detected either under UV light or by placing in an iodine chamber. Melting points were determined in open capillaries using an Electrothermal 9100 instrument. Chemical analyzes of the samples were carried out with Philips-PW1480 X-ray fluorescence (XRF). The crystalline phase of the nanoparticles was identified by means of X-ray diffraction (XRD) measurements using  $\text{Cu K}_\alpha$  radiation ( $\lambda = 1.54\text{\AA}$ ) on a Philips-PW1800 diffractometer in the  $2\theta$  range of  $4\text{--}90^\circ$ . A Netzsch Thermoanalyzer STA 504 was used for the thermogravimetric analysis (TGA) with a heating rate of  $10^\circ\text{C}/\text{min}$  under air atmosphere. Fourier transform infrared (FT-IR) spectra were recorded using Perkin-Elmer Spectrum RXI FT-IR spectrometer; using pellets of the nanomaterials diluted with KBr. The  $^1\text{H}$  NMR spectra were recorded on Bruker DRX-300 Avance spectrometer at 300.13 MHz. The elemental analyses were performed with an Elementar Analysensysteme GmbH VarioEL. Scanning electron microscopy (SEM)

images of the samples were taken with Zeiss-DSM 960A microscope with an attached camera. Magnetic susceptibility measurements were carried out using a vibrating sample magnetometer (VSM) by Megnetic Daghigh Daneshpajouh Co., Kashan, Iran, in the magnetic field range of  $-10000$  Oe to  $+10000$  Oe at room temperature. Transmission electron microscopy (TEM) images were provided by Transmission electron microscopy (TEM) analysis was performed using a Zeiss EM 900 electron microscope (Germany) operating at 80 kV. Dynamic light scattering (DLS) analysis was carried out on a Malvern Instruments Ltd. Zetasizer Ver. 6.01 (England). All products were known compounds that identified by comparison of their spectroscopic and analytical data with those authentic samples.

#### 4.2 | Preparation of $\text{Fe}_3\text{O}_4@\text{SiO}_2@\text{PPh}_3@\text{Cr}_2\text{O}_7^{2-}$ nanocatalyst

First, SPIONs were synthesized via co-precipitation method. Then,  $\text{Fe}_3\text{O}_4@\text{SiO}_2$  was prepared through a modified Stober method.<sup>[27]</sup> After that, silica coated SPIONs were functionalized with triphenylphosphine. Finally, dichromate anion was immobilized on the surface of phosphonium groups to give the functionalized magnetite composite nanoparticles.

#### 4.3 | General procedure for synthesis of polyhydroquinolines

To a mixture of an aldehyde (1 mmol), dimedone or 1,3-cyclohexadione (1 mmol), ethyl acetoacetate (1 mmol), and ammonium acetate (1 mmol) in a 10 ml round bottom flask, the magnetite nanocatalyst (0.003 g) was added. The mixture was homogenized and stirred at room temperature for the appropriate time. The progress of the reaction was monitored by TLC. After completion of the reaction, EtOAc (5 ml) was added, and the catalyst was removed from the reaction mixture by an external magnet. The pure polyhydroquinolines were obtained by recrystallization from EtOH. The recycled nanocatalyst was used for subsequent runs under the same conditions without significant loss of its catalytic activity.

#### 4.4 | Characterization data of the selected products

##### 4.4.1 | Ethyl 2,7,7-trimethyl-5-oxo-4-p-tolyl-1,4,5,6,7,8-hexahydroquinoline-3-carboxylate (**5c**)

IR (KBr) ( $\nu_{\text{max}}$ ,  $\text{cm}^{-1}$ ) = 3276, 3205, 2958, 1701, 1647, 1604, 1492, 1379, 1215, 1033.  $^1\text{H}$  NMR (300 MHz,  $\text{CDCl}_3$ ):  $\delta_{\text{H}}$  (ppm) = 0.96 (3H, s,  $\text{CH}_3$ ), 1.08 (3H, s,  $\text{CH}_3$ ), 1.26 (3H, t,

$J = 7.2$  Hz, CH<sub>3</sub>), 2.26 (3H, s, CH<sub>3</sub>), 2.22-2.34 (4H, m, 2CH<sub>2</sub>), 2.38 (3H, s, CH<sub>3</sub>), 4.16 (2H, q,  $J = 7.2$  Hz, OCH<sub>2</sub>), 5.43 (1H, s, CH), 6.19 (1H, br s, NH); 6.84 (2H, d,  $J = 7.5$  Hz, H-Ar), 7.03 (2H, d,  $J = 7.5$  Hz, H-Ar). Anal. Calcd for C<sub>22</sub>H<sub>27</sub>NO<sub>3</sub>: C, 74.76; H, 7.70; N, 3.96. Found: C, 74.71; H, 7.66; N, 4.03.

#### 4.4.2 | Ethyl 4-(4-chlorophenyl)-2,7,7-trimethyl-5-oxo-1,4,5,6,7,8-hexahydroquinoline-3-carboxylate (5d)

IR (KBr) ( $\nu_{\max}$ , cm<sup>-1</sup>) = 3274, 3205, 3076, 2960, 1704, 1647, 1604, 1488, 1380, 1278, 1215, 1070. <sup>1</sup>H NMR (300 MHz, CDCl<sub>3</sub>):  $\delta_{\text{H}}$  (ppm) = 0.93 (3H, s, CH<sub>3</sub>), 1.08 (3H, s, CH<sub>3</sub>), 1.20 (3H, t,  $J = 7.1$  Hz, CH<sub>3</sub>), 2.06-2.31 (4H, m, 2CH<sub>2</sub>), 2.38 (3H, s, CH<sub>3</sub>), 4.06 (2H, q,  $J = 7.1$  Hz, OCH<sub>2</sub>), 5.03 (1H, s, CH), 6.23 (1H, br s, NH), 7.16 (2H, d,  $J = 8.1$  Hz, H-Ar), 7.26 (2H, d,  $J = 8.4$  Hz, H-Ar). Anal. Calcd for C<sub>21</sub>H<sub>24</sub>ClNO<sub>3</sub>: C, 67.46; H, 6.47; N, 3.75. Found: C, 67.32; H, 6.54; N, 3.82.

#### 4.4.3 | Ethyl 2,7,7-trimethyl-5-oxo-4-(thiophen-2-yl)-1,4,5,6,7,8-hexahydroquinoline-3-carboxylate (5n)

IR (KBr) ( $\nu_{\max}$ , cm<sup>-1</sup>) = 3274, 3207, 2960, 1701, 1647, 1604, 1492, 1379, 1215, 1072. <sup>1</sup>H NMR (300 MHz, CDCl<sub>3</sub>):  $\delta_{\text{H}}$  (ppm) = 1.04 (3H, s, CH<sub>3</sub>), 1.10 (3H, s, CH<sub>3</sub>), 1.27 (3H, t,  $J = 7.1$  Hz, CH<sub>3</sub>), 2.22-2.34 (4H, m, 2CH<sub>2</sub>), 2.38 (3H, s, CH<sub>3</sub>), 4.16 (2H, q,  $J = 7.1$  Hz, OCH<sub>2</sub>), 5.42 (1H, s, CH), 6.19 (1H, br s, NH), 6.84 (2H, d,  $J = 1.8$  Hz, H-Ar), 7.03 (1H, t,  $J = 2.1$  Hz, H-Ar). Anal. Calcd for C<sub>19</sub>H<sub>23</sub>NO<sub>3</sub>S: C, 66.06; H, 6.71; N, 4.05. Found: C, 67.11; H, 6.63; N, 3.94.

## ACKNOWLEDGEMENTS

The authors gratefully acknowledge the partial support from the Research Council of the Iran University of Science and Technology.

## ORCID

Ali Maleki  <http://orcid.org/0000-0001-5490-3350>

## REFERENCES

- [1] A. Maleki, R. Paydar, *React. Funct. Polym.* **2016**, *109*, 120.
- [2] I. Pastan, M. M. Gottesman, *N. Engl. J. Med.* **1987**, *316*, 1388.
- [3] B. Loev, K. M. Snader, *J. Org. Chem.* **1965**, *30*, 1914.
- [4] A. C. Gaudio, A. Korokovas, Y. Takahata, *J. Pharm. Sci.* **1994**, *83*, 1110.
- [5] P. P. Mager, R. A. Coburn, A. J. Solo, D. J. Triggle, H. Rothe, *QSAR, Drug Des. Disc.* **1992**, *8*, 273.
- [6] M. F. Gordeev, D. V. Patel, E. M. Gordon, *J. Org. Chem.* **1996**, *61*, 924.
- [7] R. Miri, H. Niknahad, G. Vesal, A. Shafiee, *IL Farmaco* **2002**, *57*, 123.
- [8] A. Dondoni, A. Massi, E. Minghini, S. Sabbatini, V. Bertoasi, *J. Org. Chem.* **2003**, *68*, 6172.
- [9] M. Poliakoff, P. Licence, *Nature* **2007**, *450*, 810.
- [10] A. Maleki, E. Akhlaghi, R. Paydar, *Appl. Organometal. Chem.* **2016**, *30*, 382.
- [11] A. Maleki, M. Aghaei, N. Ghamari, *Appl. Organometal. Chem.* **2016**, *30*, 939.
- [12] A. Maleki, M. Kamalzare, *Catal. Commun.* **2014**, *53*, 67.
- [13] A. Maleki, M. Aghaei, N. Ghamari, *Chem. Lett.* **2015**, *44*, 259.
- [14] M. A. Zolfigol, R. Ayazi-Nasrabadi, S. Bagheri, *Appl. Organometal. Chem.* **2016**, *30*, 273.
- [15] A. Maleki, *Ultrason. Sonochem.* **2018**, *40*, 460.
- [16] A. Maleki, S. Azadegan, *Inorg. Nano-Met. Chem.* **2017**, *47*, 917.
- [17] A. Maleki, M. Aghaei, R. Paydar, *J. Iran. Chem. Soc.* **2017**, *14*, 485.
- [18] A. Maleki, *Tetrahedron Lett.* **2013**, *54*, 2055.
- [19] A. Maleki, *RSC Adv.* **2014**, *4*, 64169.
- [20] A. Maleki, R. Rahimi, S. Maleki, N. Hamidi, *RSC Adv.* **2014**, *4*, 29765.
- [21] A. Maleki, M. Rabbani, S. Shahrokh, *Appl. Organometal. Chem.* **2015**, *29*, 809.
- [22] R. Kardooni, A. R. Kiasat, H. Motamedi, *J. Taiwan Inst. Chem. Engin.* **2017**, *81*, 373.
- [23] A. Khazaei, A. R. Moosavi-Zare, H. Afshar-Hezarkhani, V. Khakyzadeh, *RSC Adv.* **2014**, *4*, 32142.
- [24] D. Li, J. Wang, F. Chen, H. Jing, *RSC Adv.* **2017**, *7*, 4237.
- [25] A. Maleki, M. Kamalzare, M. Aghaei, *J. Nanostruct. Chem.* **2015**, *5*, 95.
- [26] A. Maleki, A. R. Akbarzade, A. R. Bhat, *J. Nanostruct. Chem.* **2017**, *7*, 309.
- [27] A. Maleki, *Tetrahedron* **2012**, *68*, 7827.

**How to cite this article:** Maleki A, Hamidi N, Maleki S, Rahimi J. Surface modified SPIONs-Cr(VI) ions-immobilized organic-inorganic hybrid as a magnetically recyclable nanocatalyst for rapid synthesis of polyhydroquinolines under solvent-free conditions at room temperature. *Appl Organometal Chem.* 2018;e4245. <https://doi.org/10.1002/aoc.4245>